International Journal for Multidisciplinary Research (IJFMR)
E-ISSN: 2582-2160 ● Website: www.ijfmr.com ● Email: editor@ijfmr.com

Analytical Evaluation of Various Metal Complexes with 2,6-Bis (((1-Octyl-1h-1,2,3-Triazol-4-Yl) Methoxy) Methyl) Pyridine

Pallavi Sinha[1], Heena Innani[2]

[1]Research Scholar, Lords University, Alwar Rajasthan
[2]Assistant Professor, Lords University, Alwar Rajasthan

ABSTRACT
The main aim of the study is Some Metal Complexes With 2,6-Bis(((1-Octyl-1h-1,2,3-Triazol-4-Yl) Methoxy) Methyl) Pyridine. All the synthesized complexes have the capacity to have electrical conductivity, and the recommended geometries for the Mn-complex are octahedral, while the suggested geometries for the Pd and Au-complexes are square planer.The compounds exhibit potent antibacterial behavior against Escherichia coli, and their antibacterial and antifungal efficacies improve with increasing concentration and synergy, respectively.

Keywords: Plagued, Electrical, Geometries, Complexes, Octahedral, Conductivity

1. INTRODUCTION

Insect pests, weeds, and plant diseases have plagued farmers ever since they first began cultivating land. Insect pests may often be easily seen, and in some instances, eliminated by hand. Hoeing and hand weeding, a never-ending chore, helped get rid of the weeds to some extent. However, the spread of rust, powdery mildew, and smut throughout the fields was as random as their unseen adversaries. Therefore, they captivated the minds of country inhabitants, and mystical understandings of illness prevention became the norm in the pre-agricultural era. Farmers had no practical way of protecting their crops from the devastation of fungal infections prior to the discovery of Bordeaux mixture in 1880 (Butler EJ. 1918). It wasn't until very recently that scientists realized fungi were to blame for plant decline (Butler EJ. 1918). Active control was impossible save for a few heuristics aimed at preventing sickness. The societal effects of large-scale pandemics were often disastrous. Even today, we may witness the effects of the Irish potato famine of the 1840s (Liu Y. et al 2017).

1.1 Thiazole

Benzothiazole is the most significant heterocyclic molecule because of the unique methyne center found in the thiazole ring. Some benzothiazole moieties, like Riluzole, are utilized as medications (Miller RG et al 2012), and this electron-withdrawing scaffold was thermally stable and had a wide range of potential uses. The scent of tea leaves contains benzothiazole bioluminescent analogs, while taste components generated by fungus like Aspergillus clavatusand Polyporousfrondosus (Gunawardana, G.P.; Kohmoto, S.; Burres, N.S. 1989) also include this compound.

Fireflies produce luciferin, a chemical with a benzothiazole derivative structure. The presence of the luciferase enzyme causes oxidation of luciferin, leading to the release of energy in the form of light.

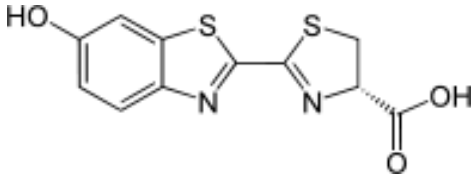

2. LITERATURE REVIEW

T. Singha, J. Singh, *et al.***[2012]** followed the procedures described in the literature to synthesis a series of 4-amino-5-mercapto-3-aryl-1,2,4-triazoles with potential bioactivity. Spectroscopic analysis was used to analyze the produced chemicals and determine whether they have anticancer action against EAC (Ehrlich ascites carcinoma). Compounds were administered intraperitoneally at a dosage of 25 milligrams per kilogram of body weight. Tumor volume, viable cell count, and tumer weight all decreased in groups, but tumer weight, ascites cell inhibition, and non-viable cell count all increased, as did median survival time. All of the compounds showed substantial anticancer activity relative to the control, and several of the compounds were found to be particularly powerful.

A series of [1,2,4]triazolo[1,5-a]pyridines weresynthesizedand characterizedby X. Wang *et al* **[2013]**. The *in vitro* antiproleferative activity was evaluated by MTT against threehuman cancer cell lines, HCT-116, U-87 MG and MCF-7. The SAR of target compoundswas preliminarily dicussed. Some of the compounds with potent antiproleferative activityweretestedfortheireffectsontheAKTandp-AKT473.Theanticancereffectwasevaluatedinmicebearingsarcoma S-180model.Theresultssuggestthatthetitlecompoundsarepotentanticanceragents.

Ying-ChaoDuan*etal*.**[2013]**synthesizedaseriesof novel 1,2,3-triazolethiosemicarbazide hybrids and their antiproleferative activity wasevaluated against four human cancer lines. The results showed that number of hybridsexhibited potent activity in selected human cancer cell lines. Among them few compoundsshowed broad spectrum anticancer activity with IC_{50} values ranging from 0.76 to 20.84mm. Evidences of cell cycle arrest and apoptosis induction were obtained for the mosteffective compounds.

OlcayBekircan*etal*.**[2015]**synthesizedaseriesof4-arylideneamino-4H-1,2,4-triazoles and 4-(1-aryl)ethylidene-4H-1,2,4-triazolesby the treatment of 4-amino-1,2,4-triazole with certain aldehydes and ketones. Compounds have been reduced with $NaBH_4$ toyield corresponding 4-arylmethylamino-4H-1,2,4-triazoles and 4-(1-aryl)ethylamino-4H-1,2,4-triazoles. The chalconeswerereacted with Thiourea in the presence of KOH in ethanol, which led to the formation of dihydropyrimidine derivatives as a beneficial antimicrobial,anticonvulsant,andanticanceragentsbyKhanage.Allthesynthesisedcompounds were screened for their *in vitro* antimicrobial activity by agar well method andtheiranticonvulsantactivitybytheMESmodel.Anticanceractivityoftwonewelysynthesised heterocycles was evaluated against 60 cell lines of different human tumer at asingle doseof10^{-5}M.

M. R. Shiradkar*et al* **[2017**], Number of articles were found for the anticonvulsant potential of 1,2,4-triazolewheresubstitutionon2,3,5positionsweredone.Recently,anticonvulsantactivityofclubbedthiazolidinone-barbituricacidandthiazolidinone-triazolederivativeshasbeenreported. 3-(2-Chloroacetyl)-2-arylimino-5-[(Z)-arylmethylidene]-1,3-thiazolan-4-onesontreatmentwith5-(1-phenoxyethyl)-4H-1,2,4-triazole-3-thiolinidenticalconditions provided a set of bulkier derivatives which have also shown the anticonvulsant potential.

Pradeep Goyal *et al*. **[2011]** synthesized some new derivatives of 3-substituted-4H-1,2,4-triazoles.All the synthesized compounds were evaluated for anti-inflammatory activity andacutetoxicity.Mostof thecompoundsshowedpotentandsignificantresultscomparedtostandardibuprofen.

The purpose of this brief review is to update the reader on the investigation of 1,2,3-triazole complexes with transition metals as possible antibacterial agents. The purpose of this article is to draw attention to existing research and to convince the reader that this underexplored area has tremendous potential for the discovery of new and more effective therapeutic compounds. After 24 hours of incubation at 37 degrees Celsius, the produced ligand and its complexes were evaluated for their biological properties as antibacterial (against Staphylococcus aureus and Escherichia coli) and antifungal (against candida albicaus) agents.

3. METHODOLOGY

3.1 SYNTHESIS AND CHARACTERIZATION OF SOME METAL COMPLEXES WITH 2,6-BIS(((1-OCTYL-1H-1,2,3-TRIAZOL-4-YL) METHOXY) METHYL) PYRIDINE

3.1.1 Materials, physical measurements, and analysis

The chemicals that were used in this research were of the highest possible purity, and they were purchased from companies such as BDH, Merck, and Sigma-Aldrich. For the determination of the (C, H, and N) contents, the Euro EA3000 analyzer was used. NMR spectra were obtained by using Bruker DPX spectrometers at a frequency of 600 MHz to collect the data. COSY and HSQC were utilized to support the NMR assignments of the target compounds. In order to obtain HRMS in the positive ion mode using an electrospray-ionization (ESI) source, the Orbitrap LTQ XL ion trap MS system. To evaluate the FT-IR spectra of the produced complexes and their ligand in the solid state in the range of wavenumber at 4000-400 and 4000-200 cm^{-1} by employing KBr and CsI pellets, an Agilent spectrometer known as the FT-IR 8400S SHIMADZU Spectrophotometer was used. The electronic spectra were acquired at wave lengths ranging from (1100-190) nm for the synthesized compounds and their ligand in solution state using a UV-Vis, 1800 PC Shimadzu Spectrophotometer. The wave lengths ranged from 100 to 190 nanometers. At a temperature of 25 degrees Celsius, both the electrical conductivity meter (WTW) and the magnetic susceptibility of complexes were measured. The GALLEN KAMP M.F.B-60 SMP30/ Stuart equipment was used to make the measurements for the melting point of all the solid products. In order to regulate the reaction, thin layer chromatography was utilized, and the silica plates that were used were (60 F254, 0.2 mm), and they carried an alkaline potassium permanganate dip.

3.1.2 Synthesis of Thiazole:

Shinde et.al. described a one pot synthesis of substituted thiazoles from styrenes with NBS in water followed by reaction with 2-aminopyridines or thioamides to afford important heterocyclic scaffold. The reaction proceeds via in-situ formation of α- bromoketone to provide imidazo pyridines and thiazoles.

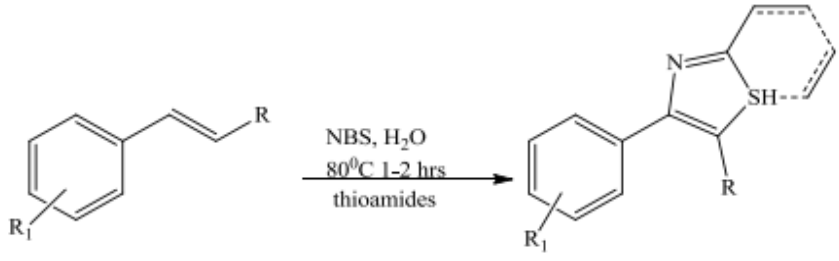

Scheme 1.1: Synthesis of thiazole derivatives from thioamides.

Cheng et.al. described the synthesis of 5-aminothiazole-4 carboxylates from thioamides upon reacting with ethyl glyoxylate and acetyl chloride via formation of corresponding imines, which on reaction with aqueous sodium cyanide, undergo a Strecker addition–cyclization reaction to yield 2-substituted ethyl 5-aminothiazole-4- carboxylates.

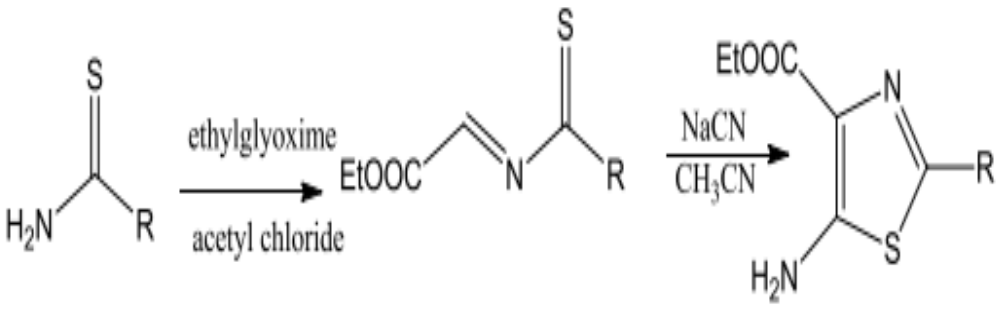

Scheme 1.2: Synthesis of thiazole derivatives from carboxylates.

3.2 Synthesis of 2,6-bis(((1-octyl-1H-1,2,3-triazol-4-yl)methoxy)methyl)pyridine [BOTMMP/L]

Preparation of this ligand was carried out according to the following steps (as shown as in Scheme 2):

A-Synthesis of n-alkyl azides (1-azidooctane) [1-AO]

After continuing to stir the formed suspension at (60-70) °C in a heated oily bath for about (5-6) hours, the mixture of reaction was poured into (140) mL of distilled water, and then it was separated by (99.8%, 350) mL of diethyl ether. The final product had a purity of 99.8%. After that, the organic layer was collected and washed to produce a liquid that was light yellow in color and contained 1-azidooctane. Following that, it was purified by flash chromatography (silica gel, n-hexane), Rf = 0.82 (n-hexane), which resulted in a white liquid being produced.

B-Synthesis of 2,6-bis((prop-2-yn-1-yloxy)methyl)pyridine[BPMP]

Before adding propargyl bromide (98%, 3.79 mL, 44 mmol) dropwise, the ice-salt bath was used to cool the round flask in (-20 °C) with agitate the contents for 10 minutes. After that, the reaction mixture was stirred for an additional 24 hours while being heated gradually at room temperature. Later, the reaction was stopped by adding one hundred milliliters (mL) of distilled water, and then fifty milliliters (mL) of ethyl acetate (at a concentration of 99.5%) was used to extract it three times to produce a light-yellow oil. Finally, the organic layer was washed with a solution of potassium chloride and distilled water. After that, Na2SO4 was used to dry it out and filter it, and the solvent was then evaporated at a low pressure. Chromatography was completed in a flash using 9:1 silica gel, n-hexane: ethyl acetate, with an Rf value of 0.75 for [BPMP] in a brilliant yellow liquid containing 2.23 grams (percent).

C-Synthesis of 2,6-bis(((1-octyl-1H-1,2,3-triazol-4-yl) methoxy) methyl) pyridine [BOTMMP/L]

[BPMP] A heterogeneous mixture consisting of (98%, 0.039 g, 0.2 mmol) of sodium ascorbate and (0.025 g, 0.01 mmol) of CuSO4.5H2O in (2) mL of DMSO was given an addition of (99%, 0.215 g, 1 mmol) of sodium ascorbate through dropwise addition to (3) mL of DMSO. Following a stirring period of two minutes, three millimoles of 1-azidooctane were added to the mixture. The mixture was heated while being stirred for a total of 48 hours at (50-60) degrees Celsius. After adding thirty milliliters of distilled water to it in order to wet it down, it was then extracted three times with DCM (99%, fifty milliliters), dehydrated with sodium hydroxide, and finally evaporated under low pressure. Following flash chromatography, the Rf value was determined to be 0.17 (silica gel, 2:1 n-hexane: ethyl acetate). The finished product has the appearance of a white solid, and it contains the chemical that was intended.

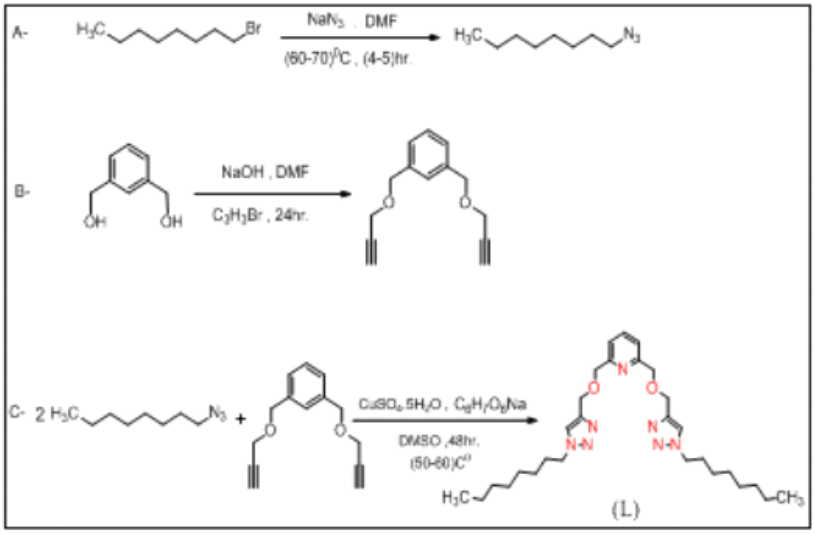

Scheme 1 steps of the synthesis of the ligand [BOTMMP/L]

4. RESULTS AND DISCUSSION

4.1 SYNTHESIS AND CHARACTERIZATION OF SOME METAL COMPLEXES WITH 2,6-BIS(((1-OCTYL-1H-1,2,3-TRIAZOL-4-YL) METHOXY) METHYL) PYRIDINE

The product was colored powders that were stable for an extended length of time when exposed to the open environment, both in their complex and chelated forms. The physiochemical characteristics of the chemicals that were produced are outlined in Table 4.1. The fact that the findings of the metal analysis match up well with the estimated values demonstrates that the analysis was accurate. The hypothesized chemical formula was supported by measurements of both the spectral and magnetic moments of the molecule.

Table 4.1 Summary of physical and analytical data for synthesized sunstances

Compounds	Color	Molecular weight g/mol	Melting point (°C)	Yield %	Elemental analysis Found (calc.) C	H	N	Metal % found (calc.)	Suggested Molecular formula
L	White	525.73	85-87	72.11	65.80 (66.20)	8.45 (9.01)	18.11 (18.65)	-	$C_{29}H_{47}N_7O_2$
L-Mn^{2+}	Light pink	669.60	169-171	71.6	51.74 (52.02)	7.17 (7.38)	14.35 (14.64)	7.95 (8.20)	$C_{29}H_{49}Cl_2N_7O_3Mn$
L-Pd^{2+}	brown	703.06	245-247	77.14	49.16 (49.49)	6.32 (6.68)	13.45 (13.94)	14.89 (15.14)	$C_{29}H_{47}Cl_2N_7O_2Pd$
L-Au^{3+}	Orang	829.06	170-172	95.7	42.27 (42.75)	5.34 (5.71)	11.29 (11.82)	23.18 (23.76)	$C_{29}H_{47}Cl_3N_7O_2Au$

4.1.1 Infrared spectroscopic study

In order to record all of the spectra in the solid state, an investigation using infrared spectroscopy with CsI discs was carried out. Based on a comparison with previously published data, FT.IR did what was anticipated of it and offered important information on the behavior of the ligand [L] with different metal ions. The chemical compound 1-azidooctane was produced by subjecting octyl bromide and sodium azide to an SN2 reaction in the presence of DMF. Strong evidence to produce the chemical 1-azidooctane can be found in the FT-IR spectra of 1-azidooctane, which can be seen in Figure 4.1. This absorption of the azide group at 2094 cm-1 is quite unique, and it can be seen in Figure 4.5. The FT-IR spectra of the chemical [BPMP] may be found shown in Figure 4.6. The reaction was successful as shown by the evanescence of a wide band at (3354) cm-1 and the appearance of sharp bands in the areas (3308 and 2121) cm-1 due to the groups (C–H and CC) of the terminal alkyne, respectively, in the FT-IR

spectra. Both regions are owing to the groups of the terminal alkyne. Bands disappearing around (2094, 2117) cm-1, demonstrating the formation of the aromatic triazole ring, and weak bands appearing at (3091, 1653) cm-1, indicating that cycloaddition reaction was successful. In addition, the spectrum of the ligand that is revealed in Figure 4.7 provides strong evidence that cycloaddition reaction was successful.

The observed bands of the free ligand L spectrum which are located in the regions (3091, 3136, 1595, 1508, 1220, and 1122) cm^{-1} that attributed to the frequencies $\upsilon(C\text{-}H)_{Pyridine}$, $\upsilon(C\text{-}H)_{Triazole}$, $\upsilon(N{=}N)_{Triazole}$, $\upsilon(C{=}N)_{Pyridine}$, $\upsilon(C\text{-}N)_{Triazole}$, and $\upsilon(C\text{-}O\text{-}C)_{Ether}$, respectively.

In the complexes, the frequency of υ (N=N) moved to increased frequency at about (4-11) cm^{-1}, while υ (C-N)Triazole, υ (C=N)Pyridine, and υ (C-O-C)Ether frequencies changed to higher frequencies at roughly (6-18), (1-51) cm^{-1}, and (31-35) cm^{-1}, respectively. The complexes of (L-Mn) exhibit novel bands for υ (Mn-N)pyridine at (271) cm^{-1} and υ (M-O) at (435-464) cm^{-1} and $\upsilon(M\text{-}N)_{triazole}$ It may be seen in the spectra of the complexes at (503-532 cm-1). In addition to (Mn-Cl), which is shown at (324) cm-1, Table 4.6 also indicates the presence of other bundles. As a direct consequence of this, we have proposed that the complexes exhibit four and six coordination geometries when they are in the solid state.

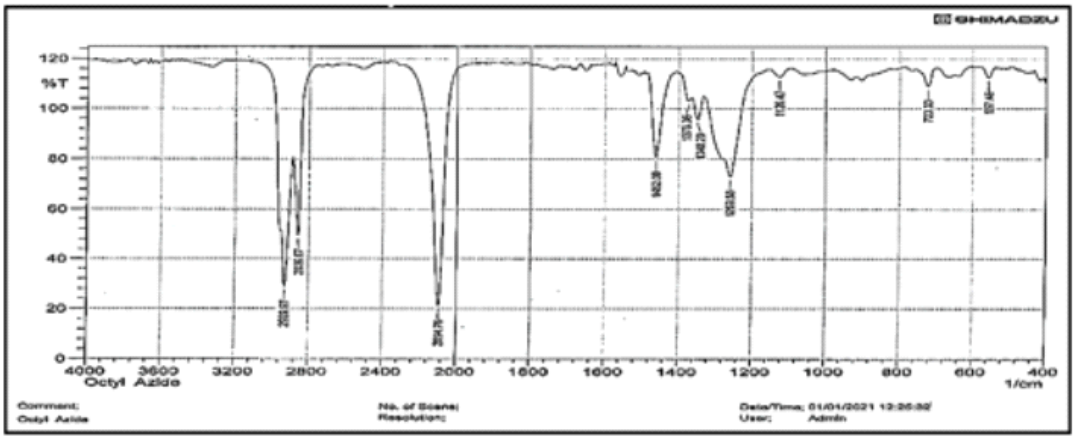

Figure 4.1 the FT-IR spectrum of 1-azidooctane compound

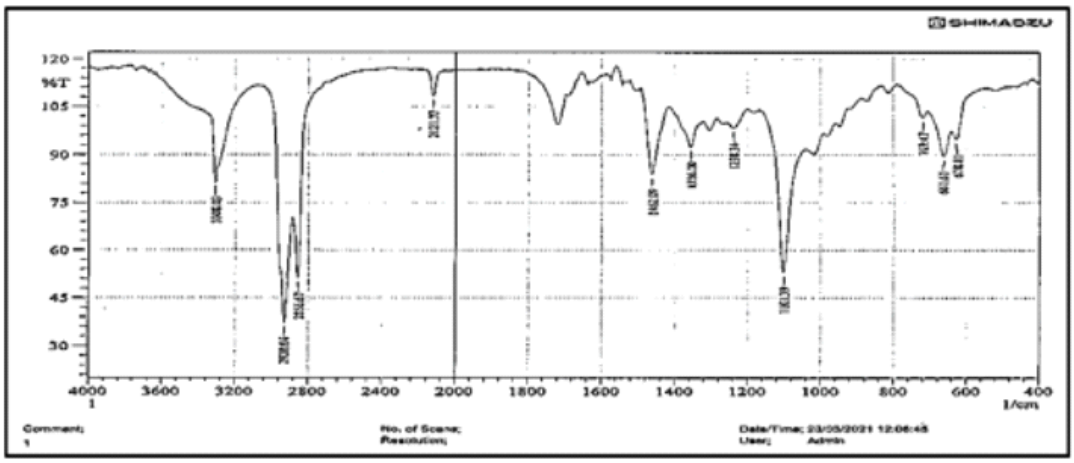

Figure 4.2 the FT-IR spectrum of [BPMP] compound

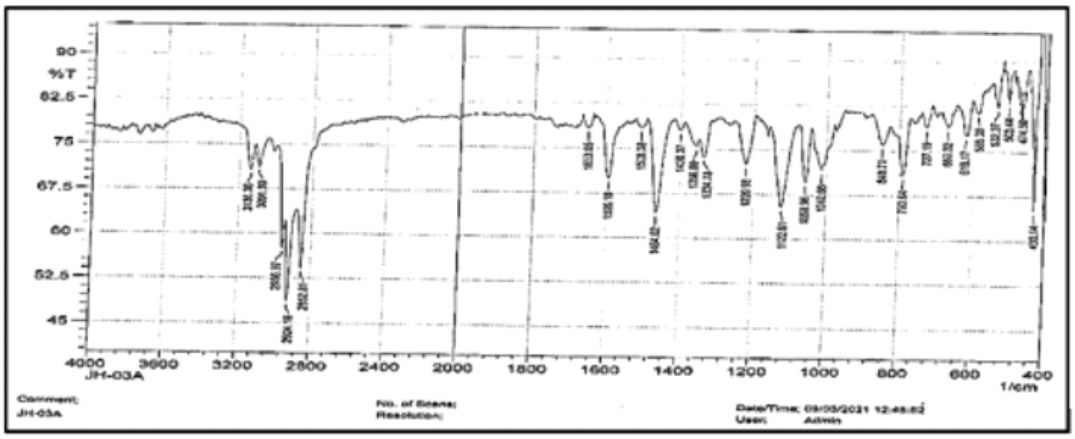

Figure 4.3 the FT-IR spectrum of [L] compound

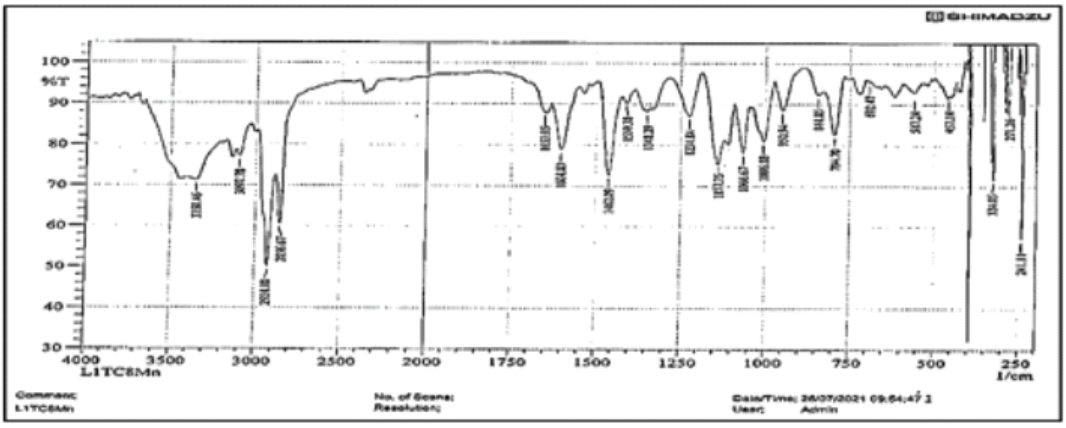

Figure 4.4 the FT-IR spectrum of prepared complex of Mn(II)

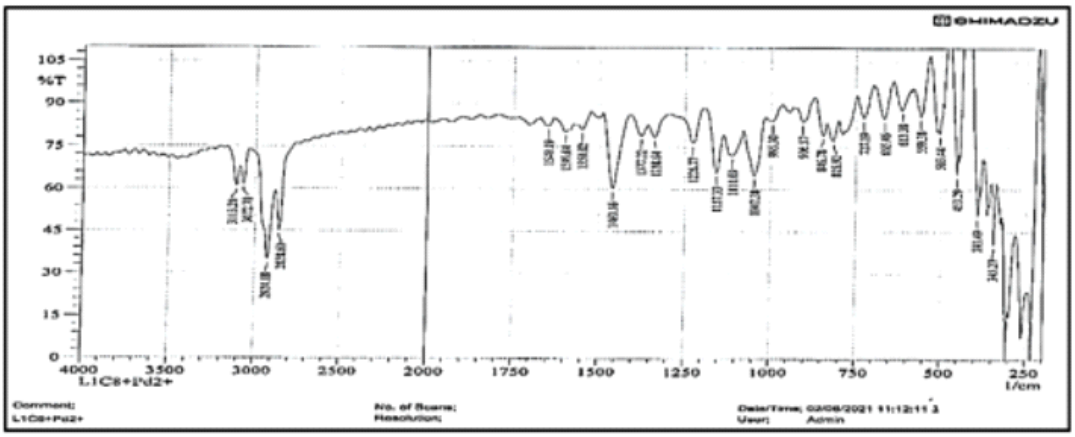

Figure 4.5 the FT-IR spectrum of prepared complex of Pd(II)

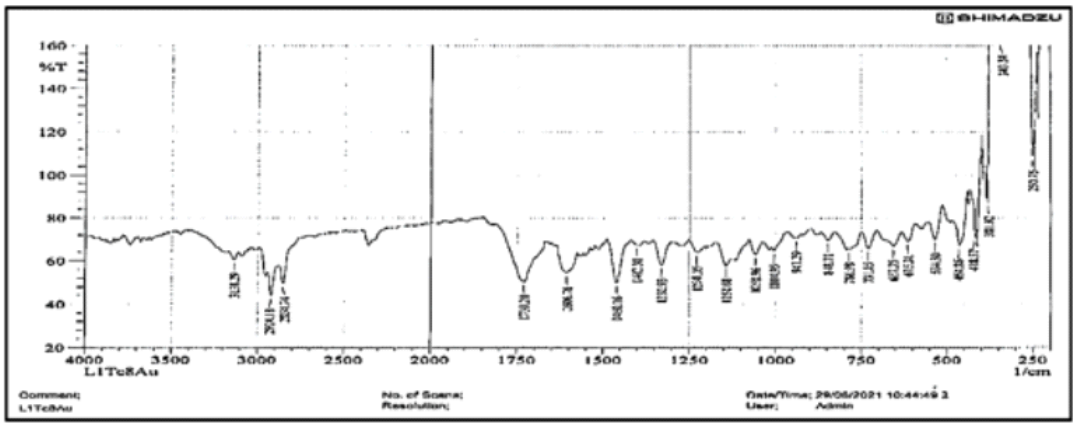

Figure 4.6 the FT-IR spectrum of prepared complex of Au(III)

Table 4.2 selected brands of FT-IR spectra of the prepared compounds in cm-1

Compound	υ(N=N) tri.	υ(C=N) py.	υ(C-N)tri	υ(C-O-C)ether	υ (M-N)py	υ(M-O)	υ(M-N) tri.	υ(M-Cl)
L	1595	1508	1220	1122	-	-	-	-
LMn	1604	1559	1234	1153	271	457	517	324
LPd	1599	1510	1226	1157	-	453	503	-
LAu	1606	1509	1238	1154	-	464	534	-

4.1.2 Measurements of conductivity, magnetic susceptibility, and electronic spectra

Additional structural tools were employed, derived from the data of electronic spectra, magnetic moments, and electrical measurements, in order to validate the geometry of the complexes that were formed. This was accomplished by using the data. The UV-Vis spectra of the complexes of the manganese, palladium, and gold ions were obtained in the range of (190-1100) nm for their solution in DMSO.

A-Spectrum of [L]

The UV-Vis spectra of ligand (L) may be seen in Figure 4.7, and it reveals that there are three bands in the ultraviolet spectrum. The first band appeared at a frequency of 42194 cm-1 as a result of an inter ligand transition to the (n→ π*) state on the pi-system. Even though it was part of a separate group, the second band of absorption occurred at 39062 cm-1 and was the same as the band that was produced from the (n→ π*) transition. The (n → π*) electronic transition point on the oxygen and nitrogen atoms were found to be responsible for the formation of the third absorption band at 37735 cm-1.

B-Spectrum of the Mn(II) complex

Light pink Mn(II) complex UV-Vis spectrum. Figure 4.8 demonstrate bands at (11235 and 26595) cm^{-1}, which back to the transitions $^6A_1g \rightarrow {}^4T_1g(G)$ (ν_1) and $^6A_1g \rightarrow {}^4A_2g + {}^4Eg(G)$ (ν_3) transitions, respectively, confirming previous research. All the parameters (10Dq, B′, the value of the band of ν_2 assigned to the $^6A_1g \rightarrow {}^4T_2g(G)$ transition, and the nepelauxetic factor) were calculated in accordance with the schematic of Tanaba and Sugano by fitting the v3/1 ratio on the diagram of the octahedral d5 structure. The ratio 3/1 =2.4 is compatible with the schematic at 1.53 Dq/B′, and the Racah parameter B' will be 714 cm-1 with a value of β=0.83 (bringing the Bo of the free ion to 860 cm-1). The value for the constant field splitting 10Dq is 10924 cm-1, which is almost identical to the value for the first transition. It has been determined that the magnetic value is 5.52 B.M., and when compared with the results of other reporters, this degree is found to relate to the octahedral geometry of the Mn (II) ion. The conductivity of this compound in DMSO at room temperature demonstrates that it has ionic properties.

The octahedral shape that surrounds the Mn (II) ion may be theorized with the use of data from spectroscopy and analysis, as shown in Table 4.3.

C-Spectrum of the Pd(II) complex:

In the UV-Vis spectrum of the brown Pd(II) complex, there are two distinct bands visible. As shown in Figure 4.9, the shoulder was the first absorption band to emerge at a frequency of 29411 cm-1, followed by the bands with a higher intensity at a frequency of 36764 cm-1. These absorption bands were assigned to the transition 1A1g →1B1g, which was represented to 10 Dq, and other 1A1g →1Eg, respectively, when the spin-parried d8 square planer arrangement was taken into consideration. This assignment required knowledge about palladium complexes that had a square planer shape, and the information was matched with data that had been published. The assessments provided by the low spin diamagnetic complex were validated by the findings that magnetic susceptibility experiments uncovered further evidence of square planer stereochemistry. Based on the results of the conductivity tests, it was determined that this substance is an electrolyte. Based on the findings and the IR spectra, which offered strong support, as shown in Table 4.7, it is possible to hypothesize that the structure of this complex has the geometry of a square planer.

D-Spectrum of the Au(III) complex

It has been shown that charge transfer bands dominate the ligand field transitions, and this information was used to determine the spectrum of the orang Au(III) ion. It follows from this that the ligand field transition will be seen at a lower wavelength, whilst the charge transfer bands will be visible at a higher wavelength. We detected two notable bands at 27027 and 34482 cm-1 in the complex gold spectra displayed in Figure 4.10. These bands correspond to the 1A1g →1B1g and 1A1g →1Eg transitions, respectively. In addition, another peak occurred at 37037 cm-1 and was ascribed to charge transfer in a square planer geometry. As can be shown in Table 4.3, the magnetic moment is equal to zero. The conductivity of this compound in DMSO at room temperature demonstrates that it has ionic properties. It has been determined via the use of spectroscopy and data analysis that this molecule has the structure of a square planer.

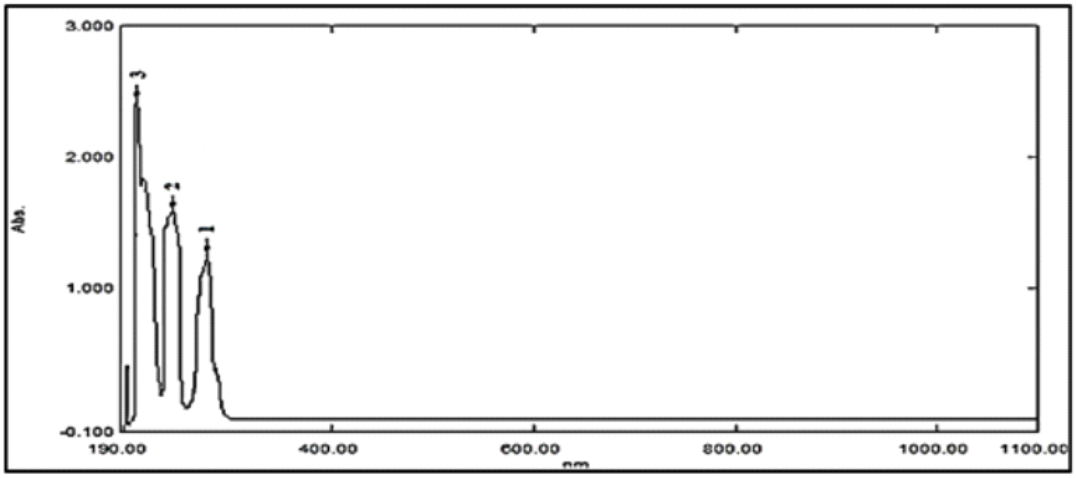

Figure 4.7 the electronic spectrum of the ligand

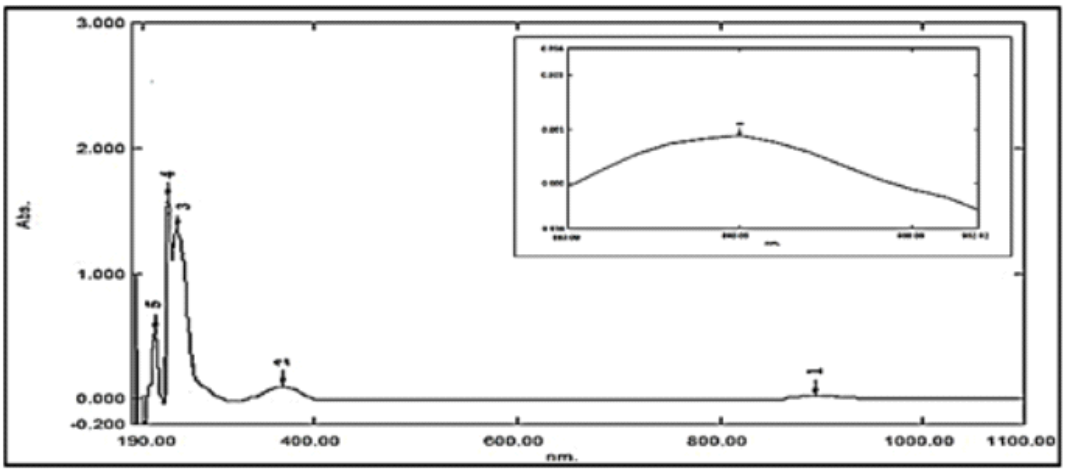

Figure 4.8 the electronic spectrum L-Mn(II)complex

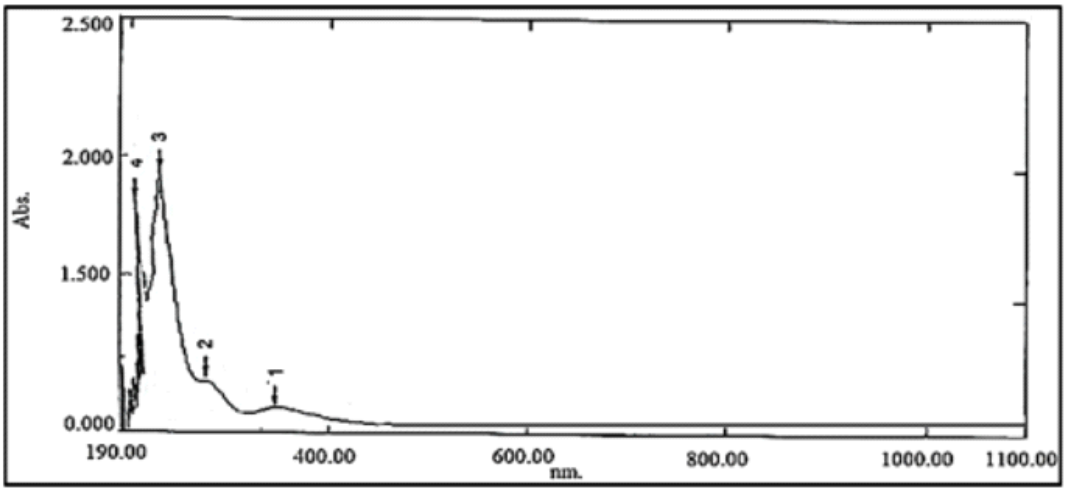

Figure 4.9 the electronic spectrum L-Pd(II)complex

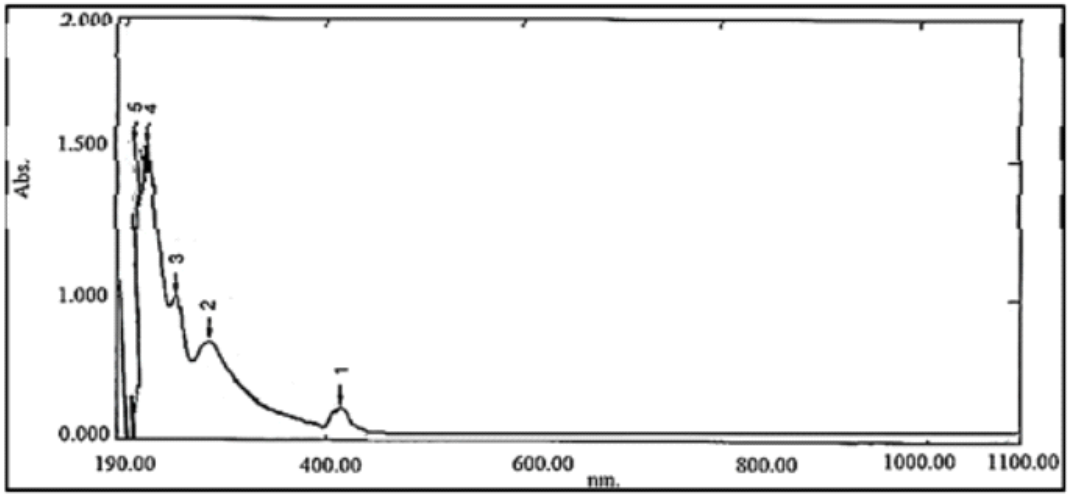

Figure 4.10 the electronic spectrum L-Au(III)complex

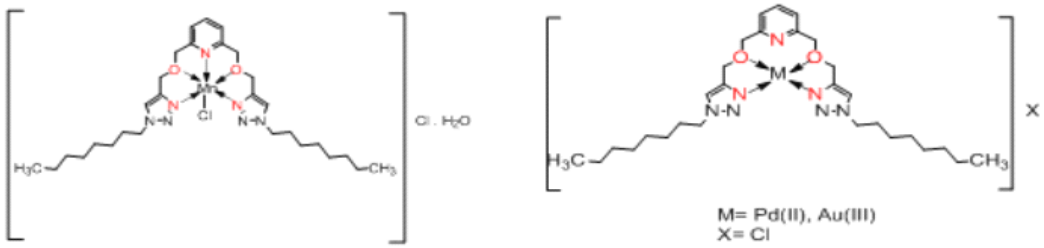

Scheme 3 proposed geometry of synthesized complexes

Table 4.3 in a DMSO solvent, complex structural insights, electronic spectroscopy data, conductivity tests, and magnetic moments

Component	Abs. cm^{-1}	Assignments	μeff B.M	μs. cm^{-1}	Suggested geometry
L	37735 39062 42194	$n \rightarrow \pi^*$ $\pi \rightarrow \pi^*$	-	-	-
L-Mn	11235 17820 26595	$^6A_1g \rightarrow {}^4T_1g_{(G)}$ $^6A_1g \rightarrow {}^4T_2g_{(G)}$ $^6A_1g \rightarrow {}^4A_2g + {}^4Eg_{(G)}$	5.52	38.2	Octahedral
L-Pd	29411 36764	$^1A_1g \rightarrow {}^1B_1g$ $^1A_1g \rightarrow {}^1Eg$	0.00	80.5	Square planer
L-Au	27027 34482 37037	$^1A_1g \rightarrow {}^1B_1g$ $^1A_1g \rightarrow {}^1Eg$ Au →LCT	0.00	297.3	Square planer

5. CONCLUSION

The data from the spectral and physical analysis indicated that the preparation of 2,6-bis(((1-octyl-1H-1,2,3-triazol-4-yl) methoxy) methyl) pyridine from starting materials was success, also the process of complexes formation using 1,2,3-triazol derivative as ligand with some light and heavy metals (Mn^{2+}, Pd^{2+} and Au^{3+}) was done with the molar ratio 1:1 of metal to ligand, where the ligand behave as tetra and penta-dentate through O and N atoms. All the synthesized complexes have the capacity to have electrical conductivity, and the recommended geometries for the Mn-complex are octahedral, while the suggested geometries for the Pd and Au-complexes are square planer. This is significant for a number of reasons, including their versatility in preparation of medicines like antibiotics, nucleosides, tri-tubercular agents, receptors, fluorinated hydrogels, chelators, surface-active agents, and radio-chemistry, and the increasing resistance to conventional antibiotics.

Square planar geometry characterizes the L-Pd and L-Au complexes, whereas octahedral geometry characterizes the L-Mn complex. All of the substances were examined at three different doses (10, 50, and 200 ppm) for their capacity to suppress the development of the chosen bacteria (Staph. aureus, and E. coli) and fungus (cand. andalbicaus). Results indicate that the compounds behave as strong antibacterial against Escherichia coli, and that increasing concentration increases activity as an antibacterial and antifungal. The gold complex was more synergistically effective than others.

REFERENCE

1. T. Singha, J. Singh, A. Naskar, T. Ghosh, A. Mandal, K. M. Kumdu, Ranjit, Harwansh, T. K. Maity, Indian J. Pharm. Educ., 2012, 46(4), 346.
2. X. Wang, J. Xu, Y. Li, H. Li, C. Jiang, G. Yang, S. Lu, S. Zhang, Eur. J. Med. Chem., 2013, 67, 243.

3. Duan YC, Ma YC, Zhang E, Shi XJ, Wang MM, Ye XW, Liu HM. Design and synthesis of novel 1,2,3-triazole-dithiocarbamate hybrids as potential anticancer agents. Eur J Med Chem. 2013 Apr;62:11-9. doi: 10.1016/j.ejmech.2012.12.046. Epub 2013 Jan 4. PMID: 23353743.
4. Bekircan Olcay, G. Nurhan, Indian J. Chem., 2015, 44B, 2107.
5. M. R. Shiradkar, A. G. Nikalje, ARKIVOC, 2017, 14, 58.
6. K. G. Pradeep, B. Anil, A. C. Rana, C. B. Jain, Asian J. Pharm. Clin. Res., 2011, 3(3), 150.
7. H. Kumar, A. Javed, Sadique, K. A. Suroor, Eur. J. Med. Chem., 2018, 43, 2688.
8. S. De Oliveira, B. F. Lira, J. M. Barbosa-Filho, J. G. F. Lorenzo, P. F. D. Athayde- Filho, Molecules, 2012, 17, 10192.
9. Trilok, G. Neha, L. Suman, S. S. Saxena, Eur. J. Med. Chem., 2011, 45, 1772.
10. H. Asif, A. Mohammed, Acta Pharm., 2019, 59, 223.
11. Mymoona, H. Asif, A. Bismillah, Eur. J. Med. Chem., 2019, 44, 2372.
12. Miller RG, Mitchell JD, Moore DH.. Riluzole for amyotropic lateral sclerosis/motor neuron disease. *Cochrane Database Syst Rev* 2012;3:CD001447.
13. Shinde, Mahesh & Kshirsagar, Umesh. (2015). One Pot Synthesis of Substituted Imidazopyridines and Thiazoles from Styrenes in Water Assisted by NBS. Green Chem.. 18. 10.1039/C5GC02771C.
14. Gunawardana, G.P.; Kohmoto, S.; Burres, N.S. New cytotoxic acridine alkaloids from two deep water marine sponges of the family Pachastrellidae. *Tetrahedron Lett.* 1989, *30*, 4359–4362.
15. Liu Y, Langemeier M, Small I, Joseph L, Fry W. Risk management strategies using precision agriculture technology to manage potato late blight. Agronomy Journal. 2017;109: 562-575
16. Butler EJ. Fungi and Disease in Plants. Calcutta: Thacker Spink and Co; 1918